JOURNAL OF VIROLOGY, Oct. 1992, p. 5832–5841
0022-538X/92/105832-10$02.00/0

Vol. 66, No. 10

# Deletions in the Hepatitis B Virus Small Envelope Protein: Effect on Assembly and Secretion of Surface Antigen Particles

REINHILD PRANGE, ROMAN NAGEL, AND ROLF E. STREECK*

*Institut für Medizinische Mikrobiologie, Johannes Gutenberg-Universität Mainz, Augustusplatz, D-6500 Mainz, Germany*

Received 18 February 1992/Accepted 1 July 1992

**The small envelope S protein of hepatitis B virus carrying the surface antigen has the unique property of mobilizing cellular lipids into empty envelope particles which are secreted from mammalian cells. We studied the biogenesis of such particles using site-directed mutagenesis. In this study, we describe the effect of deletions in the N-terminal hydrophobic and hydrophilic domains of the S protein. Whereas short overlapping deletions of hydrophilic sequences flanking the first hydrophobic domain were tolerated, larger deletions of the same sequences were not. Conversely, the hydrophilic region preceding the second hydrophobic domain was not permissive for even short deletions. Deletion of part or all of the first hydrophobic domain also completely blocked secretion, confirming that the entire apolar region serves an essential function. Most of the secretion-defective deletion mutants still entered the secretory pathway and translocated at least the second hydrophilic domain across the membrane of the endoplasmic reticulum. These mutants appeared to remain arrested in a membrane-associated configuration in the endoplasmic reticulum or the *cis*-Golgi compartment but preserved their capacity for oligomerization with the wild-type S protein. While secretion of wild-type S protein was specifically blocked by the formation of intracellularly retained mixed envelope aggregates, secretion of an unrelated protein (interleukin 9) was completely unaffected.**

During a hepatitis B virus (HBV) infection, various types of virus-related particles carrying the hepatitis B surface antigen (HBsAg) are secreted by the liver. These include complete virions (Dane particles) and spherical and filamentous particles of about 20 nm in diameter, corresponding to empty viral envelopes. The viral envelope is a complex structure composed of cellular lipids and three related viral proteins, the large, middle, and small envelope proteins. The small S protein, the predominant constituent of the envelope, is of particular interest because it has the unusual capacity to self-assemble with host-derived lipids into secreted subviral particles (14, 44).

Efforts have been made to analyze the biochemical steps that mark the biogenesis and transport of subviral particles along the exocytic pathway (5, 35, 36, 41). This process is initiated by insertion of the S protein into the membrane of the endoplasmic reticulum (ER) where it is transiently arrested in a transmembrane configuration. After aggregation of about 100 membrane-embedded S monomers, subviral particles are thought to mature by budding into the lumen of the ER. This type of budding is only poorly understood as it involves a substantial reorganization of membrane lipids (15, 39, 41). After delivery, the soluble lipoprotein particles leave the cell via the constitutive pathway of secretion.

Since no other viral proteins are required for the formation of subviral particles, the essential topogenic elements reside in the small S protein. The S protein contains three hydrophobic domains located at positions 11 to 28, 80 to 98, and 169 to 226 (19, 44) that separate two hydrophilic regions (29 to 79 and 99 to 168). Mutational analysis combined with in vitro and in vivo expression of deleted forms of the S protein has shown that both the entire first and second hydrophobic domains serve an essential function in determining protein topology (1, 5, 10, 12). While the first region mediates targeting to the ER membrane despite lacking an N-terminal-cleaved signal sequence (10, 12), the second domain seems to anchor the protein in the lipid bilayer (5, 12). In the transmembrane intermediate of the S protein, these two apolar segments are thought to span the membrane, thereby exposing the first hydrophilic region to the cytoplasmic (i.e., internal in the mature particle) and the second hydrophilic domain to the lumenal (i.e., external in the mature particle) side of the membrane (12, 41, 44). According to proposed models (16, 19) for the secondary structure of the S protein, there is consistent agreement concerning the lumenal disposition of the second hydrophilic loop since it carries the major surface antigen and acquires carbohydrate modification. Predictions for the cytoplasmic location of the first hydrophilic loop are conflicting and remain to be verified.

We have shown previously that both hydrophilic regions of the S protein tolerate various insertions of different length and sequence without effects on particle assembly and secretion (7). When heterologous epitopes were inserted, particulate HBsAg proved to be a useful immunological carrier for foreign antigens (8, 9).

We now have performed a detailed deletion mutational analysis of the N-terminal third of the S protein to identify sequences essential or dispensable for assembly and secretion of subviral particles. A set of 14 deletion mutant S proteins was analyzed by transient expression in HepG2 and COS-7 cells and characterized by various experimental approaches.

## MATERIALS AND METHODS

**Site-directed mutagenesis and molecular cloning.** Deletion mutagenesis of the S open reading frame of HBV subtype

* Corresponding author.

ayw (13) was performed according to three experimental strategies.

First, deletion mutants Δ09-22, Δ10-32, Δ22-32, Δ22-50, and Δ33-51 were constructed by using authentic restriction sites near the 5′ end of the S-coding region. To avoid multiple cutting, an *Xho*I-*Bam*HI fragment (nucleotide [nt] 129 to nt 490 of the HBV genome) carrying the N-terminal half of the S gene was first inserted in plasmid pUC18, giving rise to pUC18.S. To delete the coding sequence for amino acids 9 to 22, plasmid pUC18.S was linearized with *Sty*I (nt 180), the 5′ overlapping sequences were digested with mung bean nuclease, and the DNA was recut with *Hin*cII (nt 221). After removal of the 37-bp *Sty*I-*Hin*cII fragment, the DNA was blunt-end ligated with an 8-bp *Sal*I linker (5′-CGTC GACG-3′) to preserve the reading frame of the S gene. To exclude insertions of multiple copies of linker DNA, the plasmid obtained was digested with *Sal*I and religated. For in-frame deletion of the *Sty*I-*Xba*I (nt 249) fragment (Δ10-32), plasmid pUC18.S was cleaved with both enzymes and religated. To generate mutant Δ22-32, plasmid pUC18.S was cut with *Xba*I, made blunt by mung bean nuclease digestion, and subsequently cleaved with *Hin*cII. The junction was filled by insertion of an 8-bp *Sal*I linker, exactly as outlined for mutant Δ09-22. Mutant Δ22-50 was constructed by cleaving plasmid pUC18.S with *Hin*cII and *Bal*I (nt 305). In this mutant, one copy of a 12-bp *Nco*I linker (5′-CAGCCATG GCTG-3′) was inserted to connect the blunt-end *Hin*cII and *Bal*I restriction sites without disturbing the reading frame. For deletion of the coding sequence for amino acids 33 to 51, plasmid pUC18.S was first digested with *Xba*I. After the ends were filled in with the Klenow fragment of DNA polymerase I, the DNA was cut with *Eae*I (nt 303) and treated with mung bean nuclease. Subsequently, the flush-ended *Xba*I and *Eae*I restriction sites were religated, thereby maintaining the reading frame. The *Xho*I-*Bam*HI fragments of these recombinants carrying the deletions were then used to replace the corresponding wild-type fragment in the expression vector pLAS (7). This plasmid carries the entire S gene and its polyadenylation site (nt 47 to 1986) under the transcriptional control of the simian virus 40 early promotor.

For construction of mutants Δ01-74 and Δ10-72, a genetically engineered *Eco*RV restriction site (nt 368) was used which is located 8 bp 5′ to the methionine 75 codon of the S protein. To delete the coding sequence of the first 74 amino acid residues, an *Xho*I (nt 129)-*Acc*I (nt 827) fragment carrying the entire S gene was excised from plasmid pLAS and substituted by the shorter *Eco*RV-*Acc*I fragment. Mutant Δ10-72 was constructed in several steps to remove the *Sty*I (nt 180)-*Eco*RV (nt 368) fragment of the S gene. Briefly, after deletion of this fragment, the filled-in *Sty*I and *Eco*RV sites were religated, and the mutant gene was cloned into pLAS.

In a second approach, deletions of the S gene were created in a recombinant M13mp19 bacteriophage carrying cloned HBV DNA by the method of Nakamaye and Eckstein (31). The following oligonucleotides were used for site-directed mutagenesis:

Δ35-39 5′-GTTCCCCCTAGAAAATTCGAGTCTAGGCTCTG-3′
Δ35-46 5′-TTGGCCAAGACACACCGAGTCTAGACTCTG-3′
Δ40-46 5′-TTGGCCAAGACACACGAGAGACGTCCACCA-3′
Δ50-56 5′-GGTGAGTGATTGGAGGTAAGACACACGGTAGTT-3′
Δ57-63 5′-AAGTTGGAGGACAAGATGGGGACTGCGAATT-3′

Third, the remaining deletions were introduced by polymerase chain reaction, using "gene splicing by overlap extension" (18). This method facilitates the fusion of two DNA fragments at precise junctions irrespective of nucleotide sequences at the recombination site and without the use of restriction endonucleases. Briefly, two external primers flanking the region in which the deletion is to be created are used as well as two internal primers, each spanning the deleted sequence (see below). Each pair of external and corresponding internal primers is used in a separate polymerase chain reaction, creating two DNA fragments with identical terminal sequences. When these fragments are mixed, denatured, and reannealed, DNA strands hybridize via their terminal complementary sequences introduced by the internal primers. These strands are extended and amplified and are used to replace the wild-type sequence in pLAS. To create the deletions, plasmid pNI2 (38) carrying the entire pre-S1–pre-S2–S open reading frame was used as the template. The external primers chosen, 5′-GCTTTTGCACTC GTCCC-3′ (nt 707 to 723) and 5′-CTTGTGGCAAGG ACCC-3′ (nt 2133 to 2148), hybridize upstream and downstream of the entire S open reading frame. The internal primers are indicated below together with the corresponding amino acids of the S protein:

**E02G10**

Δ03-09 5′-CCTGCGCTGAACATGGAGGGACCCCTTCTCGTGTTA-3′
3′-GGACGCGACTTGTACCTCCCTGGGGAAGAGCACATT-5′

**P70R79**

Δ71-78 5′-TGTCCTCCAACTTGTCCTCGTTTTATCATCTTCCTC-3′
3′-ACAGGAGGTTGAACAGGAGCAAAATAGTAGAAGGAG-5′

All mutants constructed were verified by DNA sequence analysis.

**Cell culture and transfection.** Human hepatoma HepG2 HGPRT$^-$ cells (26) and COS-7 cells were cultured in Dulbecco's modified Eagle's medium supplemented with 10% fetal calf serum. For transfection, $5 \times 10^5$ HepG2 or COS-7 cells were seeded into 6-cm dishes. Unless otherwise indicated, cells were transfected with 20 μg of plasmid DNA by the calcium phosphate precipitation technique (48).

**Metabolic labeling and immunoprecipitation.** For isotopic labeling, cells were transfected as described above. Two days after transfection, the cells were washed twice with 2 ml of methionine-depleted minimal essential medium and were starved for 1 h in 1.4 ml of minimal essential medium supplemented with 1% fetal calf serum. Cells were labeled with 225 μCi of [$^{35}$S]methionine (1,186 Ci/mmol; New England Nuclear) for 24 h; during this period, the radiolabel was added in two equal portions at two time points (0 h, 12 h). After labeling, medium was collected and centrifuged at $600 \times g$ for 10 min. Cells were washed three times with ice-cold 0.1 M Tris-HCl (pH 8.0)–0.1 M NaCl and were lysed in 0.5 ml of the same buffer including 10 mM EDTA, 0.5% Nonidet P-40, 2 mM phenylmethylsulfonyl fluoride, and equal concentrations (2 μg/ml) of chymostatin, leupeptin, antipain, and pepstatin A (CLAP) for 20 min at 0°C. Lysates were clarified by centrifugation at 7,000 rpm for 10 min in an Eppendorf microcentrifuge.

For immunoprecipitation, equal portions of radiolabeled lysates and supernatants were adjusted to 0.1 M NaCl, 20 mM EDTA, 1% sodium deoxycholate, 0.5% Nonidet P-40, 0.5% Triton X-100, and 0.1% sodium dodecyl sulfate (SDS) and were incubated overnight at 4°C with rabbit antiserum to human HBsAg particles (1:100 dilution; Calbiochem). Immune complexes were isolated with a 10% (wt/vol) suspension of protein A-Sepharose (1:10 dilution; Pharmacia).

After incubation for 1 h at 4°C with rocking, the beads were washed three times with 10 mM Tris-HCl (pH 7.5)–150 mM NaCl–1% Triton X-100–1% sodium deoxycholate–0.2% SDS and then washed twice with 0.125 M Tris-HCl (pH 6.8). Proteins were eluted from Sepharose by boiling in sample buffer (50 mM Tris-HCl [pH 6.8], 2% SDS, 0.1% bromophenol blue, 10% glycerol, 5% 2-mercaptoethanol) and analyzed by electrophoresis in a 12.5% polyacrylamide gel (SDS-polyacrylamide gel electrophoresis [PAGE]). The gel was fixed, treated with Amplify (Amersham), dried, and subjected to fluorography at −70°C.

**Tunicamycin treatment and endoglycosidase analysis.** Cells were pretreated with tunicamycin (10 μg/ml; Sigma) for 2 h at 37°C before addition of the radiolabel. The drug was maintained during the labeling period.

Endoglycosidase H (endo H; Boehringer Mannheim) digestions were performed on immunoprecipitated samples. Protein A-Sepharose beads carrying bound antigen were resuspended in 20 μl of 150 mM sodium citrate (pH 5.5)–0.04% SDS–1 mg of bovine serum albumin per ml–2 μg of each ingredient of CLAP per ml. After the addition of 3 μl of endo H (1 U/μl), samples were overlaid with mineral oil and incubated for 18 h at 37°C. After removal of the oil, samples were analyzed by SDS-PAGE as outlined above.

**Velocity sedimentation of HBsAg.** HepG2 cells were transfected as described above. Three days after transfection, cellular supernatants were harvested, clarified, and subjected to ultracentrifugation for 5 h at 45,000 rpm (SW60 rotor; Beckman) and 4°C. The pellets were suspended in 10 mM Tris-HCl (pH 7.5)–150 mM NaCl–1 mM EDTA and layered on top of a 12-ml linear sucrose gradient (10 to 50% [wt/wt] sucrose in the same buffer) with a 68% sucrose cushion. After centrifugation at 35,000 rpm and 4°C for 16 h (SW40 rotor; Beckman), fractions were collected from the bottom and assayed for HBsAg by an enzyme-linked immunosorbent assay (ELISA) (Auszyme diagnostic kit; Abbott Laboratories).

**T-cell proliferation assay.** Plasmid pNI2.IL-9 carrying the entire cDNA for the mouse T-cell growth factor interleukin 9 (IL-9) (45) was transfected into COS-7 cells. After transient expression for 3 days, cellular supernatants were assayed for IL-9 secretion with ST2/K9.4a2 cells, an IL-9-dependent subclone of $CD4^+$ T-cell clone ST2/K9 that expresses a high number of IL-9 receptors. After incubation of indicator cells for 24 to 48 h with serial dilutions of the cellular supernatants of transfected cells, stimulation of T-cell growth was determined by incorporation of [$^3$H]thymidine (0.1 μCi, 3.7 kBq/$1.5 \times 10^3$ cells). Incubation was continued for another 18 h before the cells were harvested for counting. The proliferation assay was performed in the presence of neutralizing anti-mouse IL-2 and anti-mouse IL-4 antibodies (40).

**Subcellular fractionation.** COS-7 cells were transfected and metabolically labeled with [$^{35}$S]methionine as described above for HepG2 cells. After the labeling period, cells were washed and preincubated for 10 min on ice in 500 μl of 10 mM Tris-HCl (pH 7.5)–10 mM NaCl–1.5 mM $MgCl_2$–2 mM phenylmethylsulfonyl fluoride–2 μg of each ingredient of CLAP per ml. Cells were lysed by three cycles of freezing and thawing. Nuclei and unbroken cells were removed by a brief spin in an Eppendorf microcentrifuge. The postnuclear supernatant, adjusted to a final concentration of 100 mM NaCl, was separated into soluble and particulate fractions by centrifugation at 14,000 rpm for 30 min in a microcentrifuge. To extract membrane-associated proteins, the washed pellets were suspended in 500 μl of the same buffer as above including 1% Triton X-100, 0.05% sodium deoxycholate, and 0.01% SDS and incubated for 20 min on ice. After an additional centrifugation at 5,000 rpm for 5 min in an Eppendorf microcentrifuge, equal portions of the soluble and particulate fractions, adjusted to identical detergent concentrations, were analyzed by immunoprecipitation and SDS-PAGE, exactly as outlined above.

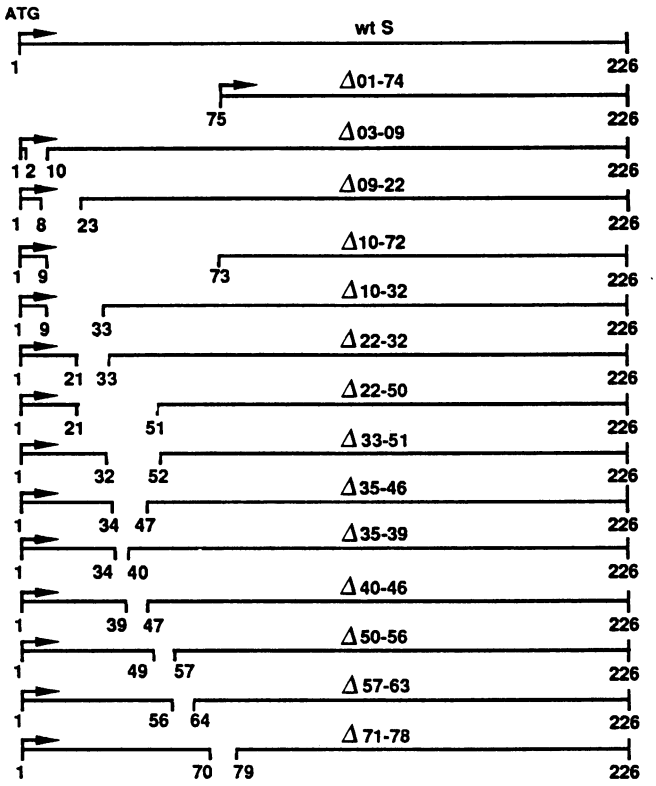


FIG. 1. Schematic diagram of the wild-type (wt) S protein of HBV and the deletion mutants analyzed in this work. The top line indicates the wild-type S protein encoding 226 aa. The following lines represent the various mutants which are named according to the amino acid sequences deleted. The gaps indicate the deletions introduced, and the numbers denote the amino acids flanking each deletion. The arrow indicates the methionine codon used for translational initiation.

## RESULTS

**Construction of S deletion mutants.** Leaving the essential hydrophobic region (amino acid [aa] 80 to 98) (5), the antigenic region (aa 99 to 168), and the C-terminal region (aa 169 to 226) unchanged, we progressively deleted sequences of variable length from the N-terminal third of the S protein using various experimental strategies (see Materials and Methods).

Although the S protein lacks an N-terminal-cleaved signal sequence (10, 12), the very N terminus of S might affect its entry into the secretory pathway. Addressing this question, we deleted aa 3 to 9 preceding the first hydrophobic region in mutant Δ03-09 (Fig. 1).

For in-frame deletion of the entire first hydrophobic domain of S, the *Sty*I-*Xba*I region of the S gene was excised in mutant Δ10-32. To analyze the topogenic elements of this segment in more detail, we constructed two mutants lacking either the N-terminal (Δ09-22) or the C-terminal (Δ22-32) part of the first hydrophobic region (Fig. 1).

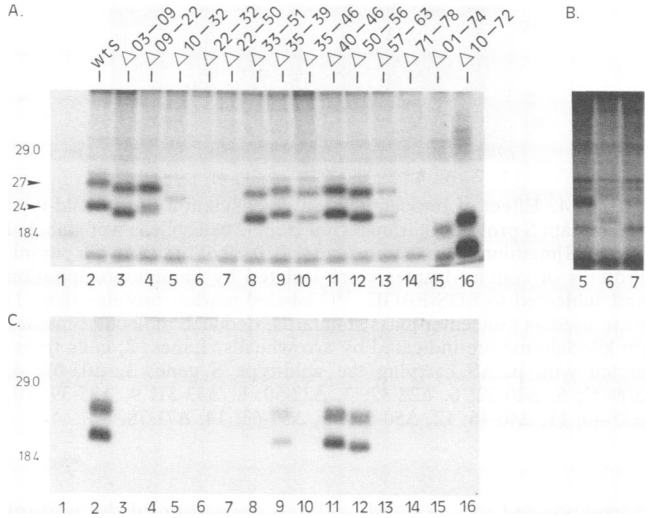


FIG. 2. Synthesis and secretion of wild-type and mutant S proteins with HepG2 cells. Transfected cells were labeled with [$^{35}$S]methionine for 24 h. Equal portions of cellular lysates (A) or cellular supernatants (C) were precipitated with rabbit antiserum against HBsAg particles and subjected to SDS-PAGE. $^{14}$C-labeled marker proteins (lanes 1) (GIBCO BRL) were used as molecular mass standards; deduced molecular masses (in kilodaltons) are indicated by arrowheads. (B) Prolonged exposure of the corresponding part of the autoradiogram shown in panel A.

To explore the function of the first hydrophilic loop for protein topology, assembly, and transport, we introduced lesions of different size into this region. In mutant Δ22-50, the N-terminal part of the first hydrophilic loop was deleted together with hydrophobic residues of the apolar segment, whereas the deletion was restricted to hydrophilic sequences in mutant Δ33-51. Similarly, mutant Δ35-46 lacks the first region of the hydrophilic loop. However, in contrast to mutant Δ33-51, the highly conserved aspartic acid residue in position 33, as well as the cysteine residue in position 48 which was found to be critical for secretion (43), was maintained in mutant Δ35-46. Subsequently, shorter deletions of this region were created, leading to mutants Δ35-39 and Δ40-46. Deletions of similar size were progressively introduced further downstream in the hydrophilic region, generating mutants Δ50-56, Δ57-63, and Δ71-78. Finally, the entire first hydrophobic and hydrophilic domains of S were removed in mutants Δ01-74 and Δ10-72 (Fig. 1).

**Synthesis of S deletion mutants.** To study the mutant proteins, we analyzed transient expression of the wild-type and mutant S genes in HepG2 cells using immunoprecipitation with polyclonal antiserum to HBsAg particles from human serum and SDS-PAGE.

Lysates of cells transfected with the wild-type S gene contained the 24-kDa nonglycosylated and the 27-kDa glycosylated forms of the small envelope protein (17) (Fig. 2A, lane 2). As shown in the same figure, all but one mutant protein (Δ71-78) could be identified in lysates of transfected cells. At least two forms of each deletion mutant were specifically immunoprecipitated (Fig. 2A, lanes 3 to 16). Consistent with the predicted molecular weights, they most likely correspond to the glycosylated and nonglycosylated forms of the mutant proteins (see also below). For the majority of the deletion mutants, the ratios of glycosylated to nonglycosylated forms were similar to those for the wild-type S protein. However, in mutants Δ09-22 (Fig. 2A, lane 4) and Δ10-32 (Fig. 2A, lane 5), both lacking the N-terminal part of the first hydrophobic domain, the ratio of glycosylated to nonglycosylated polypeptides, respectively, was increased compared with wild-type S (Fig. 2A, lane 2). Thus, deletion of this region seemed to affect the accessibility of the glycosylation site residing in the second hydrophilic loop (Asn-146). Besides the altered degree of glycosylation, mutant Δ09-22 showed additional unexpected features. First, while the glycoprotein of this mutant had a molecular mass of about 25.8 kDa, as expected, the apparent molecular mass of about 24 kDa for the nonglycosylated form was not in accord with the predicted molecular mass of about 22.8 kDa (Fig. 2A, lane 4). And second, lysates of cells transfected with this mutant contained a third immunoreactive polypeptide of about 18 kDa (Fig. 2A, lane 4).

The intracellular amounts of the mutant proteins varied and depended on the sequence deleted. Strikingly, the level of the mutant proteins Δ10-32, Δ22-32, and Δ22-50 was significantly decreased (Fig. 2A, lanes 5, 6, and 7, respectively) compared with wild-type S (Fig. 2A, lane 2). Therefore, a prolonged exposure of this part of the autoradiograph is shown in Fig. 2B. Since in all these mutants the C-terminal part of the first hydrophobic domain (aa 22 to 32) was missing, this region might have profound effects on overall stability, conformation of the surface antigen, and/or the efficiency of translocation across the ER membrane. However, when this sequence was deleted together with the entire first hydrophobic and hydrophilic region in mutants Δ01-74 and Δ10-72, the intracellular level of the mutant proteins was found to return to normal (Fig. 2A, lanes 15 and 16). In addition, the degree of glycosylation of these two mutants was not significantly altered compared to wild-type S (Fig. 2A, lane 2).

Mutant Δ71-78 carrying a deletion distal to the second hydrophobic region failed to be detected under the assay condition used (Fig. 2A, lane 14). Even during short pulse-labeling, this mutant could not be identified (data not shown).

**Secretion of S deletion mutants.** To analyze the secretory phenotypes of the deletion mutants, we immunoprecipitated cellular supernatants of transfected cells as outlined above. As shown in Fig. 2C, 4 of 14 mutants were competent for secretion. Deletion of the very N terminus of the S protein still allowed secretion (Δ03-09, Fig. 2C, lane 3; the corresponding bands are only weakly visible in the autoradiogram shown), although at a reduced level compared with wild-type S (Fig. 2C, lane 2). In contrast, secretion of mutants lacking part or all of the first apolar region was completely blocked (Δ09-22, Δ10-32, Δ22-32, and Δ22-50; Fig. 2C, lanes 4, 5, 6, and 7, respectively). Similarly, deletion of the N-terminal part of the first hydrophilic loop prevented the extracellular release, as shown by mutants Δ33-51 and Δ35-46 (Fig. 2C, lanes 8 and 10). Interestingly, secretion was restored when the amino acid sequence 35 to 46 was deleted in two parts (Δ35-39 and Δ40-46; Fig. 2C, lanes 9 and 11). In addition, an overlapping lesion of this region (aa 37 to 43) did not interfere with secretion (unpublished data). Mutant Δ50-56 was also secreted with high efficiency (Fig. 2C, lane 12), whereas mutant Δ57-63 carrying a deletion of the same size was retained intracellularly (Fig. 2C, lane 13). Large deletions covering almost the entire N-terminal third of S completely blocked secretion, as demonstrated by mutants Δ01-74 and Δ10-72 (Fig. 2C, lanes 15 and 16, respectively). Taken together, only small deletions of hydrophilic se-

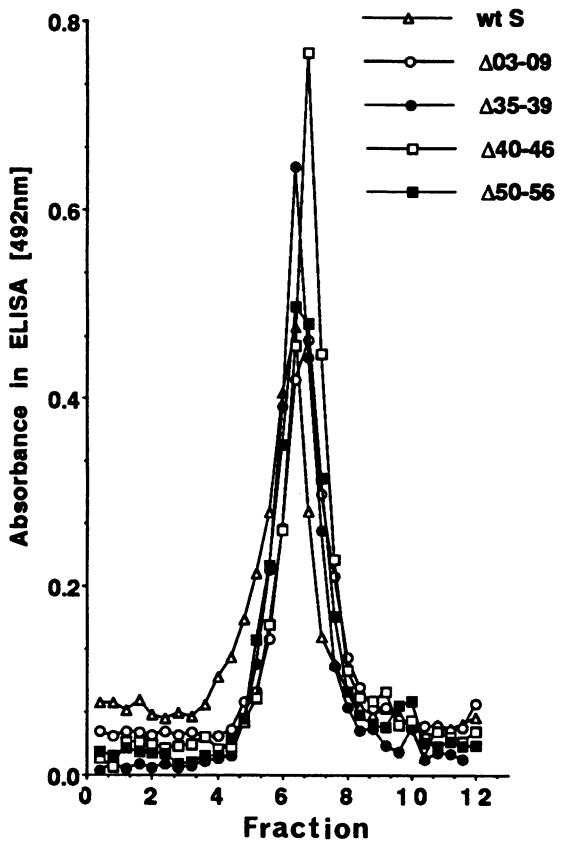


FIG. 3. Velocity sedimentation analysis of the wild-type S protein and the secretion-competent S deletion mutants Δ03-09, Δ35-39, Δ40-46, and Δ50-56. Concentrated cell culture media of transfected HepG2 cells were analyzed by sucrose gradient centrifugation. Gradients were fractionated from the bottom, and each fraction was assayed for HBsAg particles by ELISA. wt, wild type.

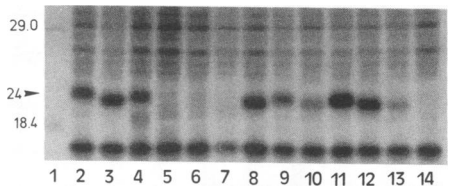


FIG. 4. Effect of tunicamycin on glycosylation of the wild-type and mutant S proteins in transfected HepG2 cells. Cells were labeled with [$^{35}$S]methionine in the presence of 10 μg of tunicamycin per ml. Proteins of cellular lysates were isolated by immunoprecipitation and subjected to SDS-PAGE. $^{14}$C-labeled marker proteins (lane 1) were used as molecular mass standards; deduced molecular masses (in kilodaltons) are indicated by arrowheads. Lanes: 2, cells transfected with pLAS carrying the wild-type S gene; 3, Δ03-09; 4, Δ09-22; 5, Δ10-32; 6, Δ22-32; 7, Δ22-50; 8, Δ33-51; 9, Δ35-39; 10, Δ35-46; 11, Δ40-46; 12, Δ50-56; 13, Δ57-63; 14, Δ71-78.

quences were compatible with the secretion of mutant S proteins.

**Characterization of secretion-competent S deletion mutants.** To determine whether the secreted deletion mutants Δ03-09, Δ35-39, Δ40-46, and Δ50-56 resemble authentic HBsAg particles, we fractionated concentrated cell culture media of transfected cells by sucrose gradient velocity sedimentation and analyzed them by an HBsAg-specific ELISA. As diagrammed in Fig. 3, the sedimentation profiles of the four mutants and the wild-type S were nearly coincident.

In addition, these mutants banded at a buoyant density of about 1.19 g/cm$^3$ in cesium chloride (data not shown), which is typical of serum-derived HBsAg particles (42). Thus, deletion of aa 3 to 9, 35 to 39, 40 to 46, or 50 to 56 affected neither proper particle assembly nor particle size of HBsAg.

**Analysis of carbohydrate modification and structure.** In an attempt to characterize the transport defects of the intracellularly retained deletion mutants in more detail, we analyzed their modification with carbohydrates. Evidence for glycosylation of the mutants was obtained after transient expression in the presence of tunicamycin. Inhibition of N-linked glycosylation yielded only the faster-migrating polypeptides in an SDS-polyacrylamide gel of the wild-type S (Fig. 4, lane 2) and the deletion mutants (Fig. 4, lanes 3 to 14). Even the 18-kDa polypeptide of mutant Δ09-22 could be detected under these conditions (Fig. 4, lane 4), indicating that it corresponded to a nonglycosylated derivative of the mutant protein. On the basis of these data, the upper bands of the immunoreactive polypeptides (Fig. 2) should therefore correspond to the glycosylated forms of the deletion mutants. Since the secretion-defective mutants were glycosylated at least as efficiently as the wild-type S (Fig. 2), insertion of these polypeptides into the ER membrane had not been impaired. Therefore, secretion of these mutants must have been blocked at a subsequent step of vesicular transport.

To investigate further the intracellular fate of the secretion-defective mutants, we analyzed the type of oligosaccharides present on the glycoproteins. Since carbohydrate modification occurs in specific subcellular compartments, transport can be monitored indirectly by determining changes in the carbohydrate structure. We therefore examined the acquisition of resistance of carbohydrate chains to endo H, an event that occurs only after modification by medial Golgi apparatus-associated enzymes. To this aim, immunoprecipitated cellular proteins were digested with endo H. All secretion-defective mutants were uniformly sensitive to treatment with this enzyme, as predominantly the nonglycosylated forms could be detected (Fig. 5A, lanes 3, 4, 5, 6, 7, 9, 12, and 13; not shown for mutants Δ01-74 and Δ10-72). The minor amounts of residual glycoproteins were attributed to incomplete enzymatic digestion. From these data, we conclude that the block to secretion of these mutants occurs before transport to the medial cisternae of the Golgi apparatus.

However, as shown in the same figure, cell-associated wild-type S (Fig. 5A, lane 1) and the secretion-competent deletion mutants (Fig. 5A, lanes 2, 8, 10, and 11) were similarly susceptible to endo H. Since the secreted glycoproteins were endo H resistant (Fig. 5B, lanes 1, 2, 8, 10, and 11), these proteins have traversed the Golgi cisternae. Concomitant to oligosaccharide processing, the molecular masses of the secreted glycoproteins increased by about 1 kDa (compare Fig. 5A and B, lanes 1, 2, 8, 10, and 11). A rapid transport through the Golgi apparatus and from the trans-Golgi apparatus to the cell surface is thought to account for the endo H sensitivity of cell-associated wild-type S (36).

**Analysis of the oligomerization capacity of secretion-defective S deletion mutants.** After insertion of S monomers into the membrane of the ER, oligomerization of S monomers appears to be the next event in the biosynthesis of HBsAg particles (41). To analyze whether the intracellularly retained mutants still preserved the capacity for intermolecular

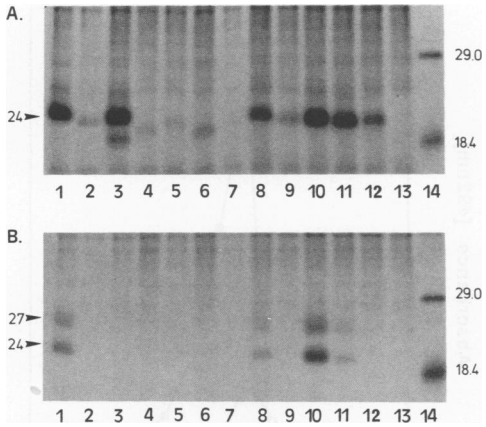


FIG. 5. Analysis of the N-linked oligosaccharides on wild-type and mutant S proteins. HepG2 cells transfected with pLAS carrying the wild-type S gene (lanes 1), Δ03-09 (lanes 2), Δ09-22 (lanes 3), Δ10-32 (lanes 4), Δ22-32 (lanes 5), Δ22-50 (lanes 6), Δ33-51 (lanes 7), Δ35-39 (lanes 8), Δ35-46 (lanes 9), Δ40-46 (lanes 10), Δ50-56 (lanes 11), Δ57-63 (lanes 12), and Δ71-78 (lanes 13) were labeled with [$^{35}$S]methionine. Cellular lysates (A) or supernatants (B) were immunoprecipitated with antiserum to HBsAg particles and digested with endo H. Proteins were separated on SDS–12.5% polyacrylamide gels. $^{14}$C-labeled marker proteins (lanes 14) were used as molecular mass standards. Deduced molecular masses (in kilodaltons) are indicated by arrowheads.

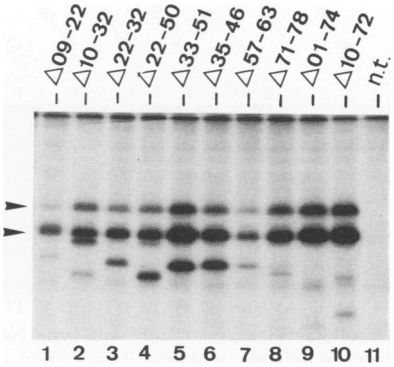


FIG. 6. Coimmunoprecipitation of a modified S protein carrying a poliovirus type 1 VP1 neutralizing epitope (9) and the secretion-deficient S deletion mutants. Each of the indicated mutant genes was cotransfected with the modified S gene at a molar ratio of 4:1, respectively. [$^{35}$S]methionine-labeled proteins from the lysates of transfected COS-7 cells were immunoprecipitated with the poliovirus-specific mouse monoclonal antibody C3 (9) and subjected to SDS-PAGE. Nontransfected (n.t.) cells were included as a control. The molecular masses of the glycosylated and nonglycosylated forms of the hybrid S-poliovirus protein of 28.5 and 25.5 kDa, respectively, are indicated by arrowheads.

aggregation, we individually cotransfected the mutant genes with the wild-type S gene at a molar ratio of 4:1, respectively. In parallel experiments, cells were transfected with the equivalent amount of the wild-type S gene alone adjusted with carrier DNA (pSVneo). The wild-type S protein was almost completely trapped within the cells when coexpressed with mutants Δ09-22, Δ10-32, Δ22-32, Δ22-50, Δ33-51, Δ35-46, and Δ57-63 (Table 1). Even mutant Δ71-78 blocked secretion of S (Table 1), indirectly indicating the synthesis of the corresponding protein. However, mutant Δ01-74 did not significantly affect secretion of wild-type S, while mutant Δ10-72 impaired but did not totally prevent the extracellular release of S (Table 1).

To demonstrate that the intracellular retention of the wild-type S protein was due to specific interaction with the mutant S proteins, epitope tagging of S was used in cotransfection experiments. The plasmid pBAP (9) encodes a modified S gene carrying an 11-aa insertion corresponding to a neutralization epitope of poliovirus type 1 VP1. Neither assembly nor secretion of envelope particles is affected by the poliovirus insertion (9). Cotransfection of pBAP with the mutant S genes was performed in COS-7 cells since we had observed a higher level of expression in these cells compared with HepG2 cells during our experiments. Assembly and secretion were virtually identical in both cell lines. When lysates of cotransfected cells were analyzed with the poliovirus-specific monoclonal antibody C3 (9), coimmunoprecipitation was found (Fig. 6), indicative of the formation of mixed envelope aggregates. The amounts of the mutant proteins Δ10-32, Δ22-32, and Δ22-50 seemed to be increased by coexpression with the modified S protein (compare Fig. 1, lanes 5, 6, and 7, and Fig. 6, lanes 2, 3, and 4). Similarly, mutant Δ71-78, which was undetectable when expressed alone (Fig. 1, lane 14), could be identified in mixed aggregates (Fig. 6, lane 8). This suggests that the mutants were stabilized by the co-oligomerization with the S protein, thereby restricting the extracellular release of S (Table 1). Conversely, the mutants Δ01-74 and Δ10-72, which had little effect on the extracellular release of S (Table 1), were found at a reduced level in mixed envelope aggregates (Fig. 6, lanes 9 and 10) compared with the amount of these proteins when expressed alone (Fig. 1, lanes 15 and 16). Thus, the level of inhibition of secretion of wild-type S by the mutants (Table 1) seems to depend on their capacity for oligomerization with the wild-type or the modified S chains.

TABLE 1. Coexpression of S deletion mutants and wild-type S protein in transfected HepG2 cells

| Plasmid + wild-type S | Secreted HBsAg |
|---|---|
| pSVneo | ++ |
| Δ01-74 | ++ |
| Δ09-22 | − |
| Δ10-72 | + |
| Δ10-32 | − |
| Δ22-32 | − |
| Δ22-50 | − |
| Δ33-51 | − |
| Δ35-46 | − |
| Δ57-63 | − |
| Δ71-78 | − |

To analyze whether the block to secretion was specific for S or due to some unspecific effect on the cellular protein secretion machinery, we assayed secretion of an unrelated protein in the presence of the mutant S proteins. We chose to study synthesis and secretion of the mouse T-cell growth factor IL-9 in COS-7 cells. When equivalent amounts of plasmids encoding IL-9 and the mutant S genes, respectively, were cotransfected at a ratio at which secretion of IL-9 was not saturated, none of the secretion-deficient mutants affected export of IL-9, as determined by an IL-9-specific T-cell proliferation assay (40) (data not shown).

**Analysis of the assembly competence of secretion-defective S deletion mutants.** To analyze whether the secretion-defective mutants still assemble into mature lipoprotein particles, we

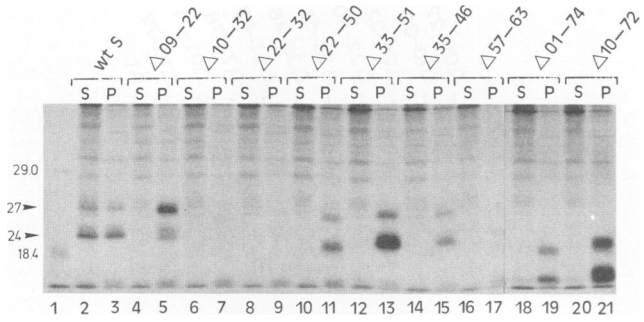


FIG. 7. Intracellular location of the wild-type (wt) S and the secretion-deficient S deletion mutants. Transfected and metabolically labeled COS-7 cells were disrupted by freezing and thawing. The postnuclear supernatants were separated into soluble (S) and particulate (P) fractions by centrifugation. Equal portions of each fraction were subjected to immunoprecipitation and analyzed by SDS-PAGE. $^{14}$C-labeled marker proteins (lane 1) were used as molecular mass standards; deduced molecular masses (in kilodaltons) are indicated by arrowheads.

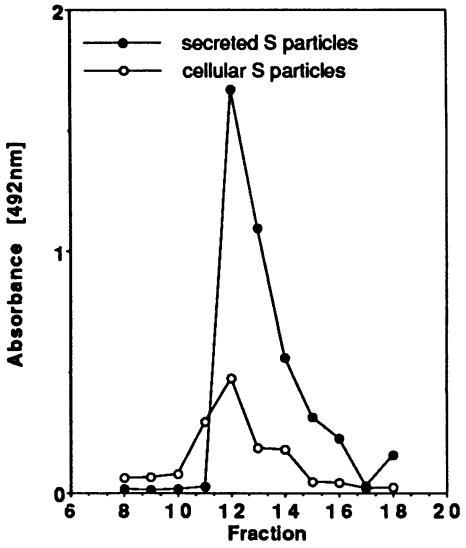


FIG. 8. Velocity sedimentation analysis of secreted and intracellular wild-type S proteins. Transfected HepG2 cells were disrupted by freeze-thaw lysis in the absence of detergents and were separated into soluble and particulate fractions (Materials and Methods). The soluble protein fraction (○) or concentrated cellular supernatants (●) were subjected to sucrose gradient centrifugation. Gradients were fractionated from the top, and each fraction was assayed for HBsAg by ELISA.

performed a subcellular fractionation experiment. Transfected and metabolically labeled COS-7 cells were disrupted by freezing and thawing, and cleared lysates were separated into soluble and particulate fractions by centrifugation. After detergent extraction of the particulate fraction, equal portions of each fraction were subjected to immunoprecipitation. During biogenesis of HBsAg particles, wild-type S still in association with the ER membrane should be insoluble in the absence of detergents, and S in the form of a lipoprotein particle should be soluble unless the centrifugation conditions employed were sufficient to pellet these particles with a sedimentation coefficient of 42S (42). Thus, the wild-type S should be distributed between the soluble and the particulate fractions after mechanical disruption of cellular organelles. As shown in Fig. 7 (lanes 2 and 3), one-half of the wild-type S was membrane associated, while the other half was soluble. The glycosylated forms of the wild-type S of each fraction displayed the same electrophoretic mobility (Fig. 7, lanes 2 and 3), implying that oligosaccharide processing had not yet occurred. Most importantly, the secretion-defective mutants were exclusively found in the membrane-associated, particulate fractions (Fig. 7, lanes 5, 7, 9, 11, 13, 15, 17, 19, and 21). These data indicate that the mutants were retained intracellularly in a membranous configuration either embedded in or tightly associated with the lipid bilayer.

The proper assembly of cell-associated wild-type S into lipoprotein particles was demonstrated further by sedimentation velocity analysis of the soluble fraction derived from mechanically disrupted cells as outlined above. No significant difference according to sedimentation in sucrose could be detected between the cell-associated soluble and the secreted forms of wild-type S (Fig. 8). The intracellular S protein present in the soluble fraction therefore appeared to be correctly assembled into envelope particles.

## DISCUSSION

In this study, we mapped subdomains of the small envelope S protein of HBV that are essential or dispensable for the assembly and secretion of subviral particles. Our detailed mutational analysis demonstrates that the N-terminal third of the S protein tolerates only minor structural lesions without affecting proper particle assembly and transport. As a main outcome of our analysis, deletions of hydrophilic segments appear to be more permissive than deletions of hydrophobic sequences.

The N-terminal half of the first hydrophilic region spacing the two apolar domains (aa 11 to 28 and 80 to 98) proved to be the most favorable site for truncations. A major factor determining retention or secretion of the mutant proteins was the length of the deleted sequence. Division of lesion 35 to 46, which entirely blocked secretion, into two parts restored transport competence (Δ35-39 and Δ40-46). Since an additional mutant of similar size lacking an overlapping segment (aa 37 to 43) was also secreted with high efficiency (unpublished results), retention of mutant Δ35-46 was not due to the absence of specific topogenic elements.

The simplest model to explain the different secretory phenotypes of these mutants is that proper folding of the S protein, a prerequisite for oligomerization and assembly (20), may require a minimum space between the two apolar domains. Similarly, extensions of the first hydrophilic region have been shown to be size limited. While in-frame insertions of various foreign sequences of 8 (7), 13 (9), or 20 (5) aa only moderately affected particle release, insertion of 23 residues completely blocked the secretion of the modified particles (5). Recent studies suggest that specific inter- or intramolecular interactions occur between membrane-spanning α-helices of transmembrane proteins (3, 29). Direct contacts between the two apolar segments of the S protein may also play a role in stabilizing the structure and promoting oligomerization and assembly. Since the relative positions of these two hydrophobic domains are determined by the length of the first hydrophilic loop, a critical number of residues may be necessary to maintain protein topology and to facilitate interactions.

Small deletions of similar size were not tolerated throughout all the first hydrophilic loop of the S protein since

mutants Δ57-63 and Δ71-78 failed to be secreted. To account for the transport defect of these mutants, we considered the deletion of the highly conserved, positively charged histidine and arginine residues, respectively. Positively charged residues preceding hydrophobic domains have been found to be important elements in determining topology and orientation of transmembrane proteins (4). According to the "positive-inside rule" of von Heijne (46), hydrophobic sequences orient themselves in the membrane with the most positively charged end in the cytoplasm. Removal of the charged residues in several integral membrane proteins either inverted their topology (33, 47) or converted them into secretory proteins (24, 34). The cluster of positively charged residues located at the junction of the first hydrophilic and the second hydrophobic domains of S may serve a similar function (21a). Our failure to detect mutant Δ71-78 lacking two arginine residues using antibodies to HBsAg particles supports this notion. However, this mutant could be rescued by oligomerization with the wild-type S or a secretion-competent modified version of S.

Our data are consistent with previous results indicating that the entire first hydrophobic domain of the S protein carries an essential topogenic element (5, 12). Neither part nor all of this region could be deleted without deleterious effects on assembly and secretion. As evidenced by glycosylation, these mutants still entered the secretory pathway, where they were arrested in a membrane-associated configuration. Targeting to and anchoring in the ER membrane of these mutants were most likely mediated through the second hydrophobic domain of S. As shown by several experiments, internal signal sequences and stop-transfer sequences can functionally substitute for each other (25, 49). Whether the use of the second hydrophobic domain for membrane targeting is a unique feature of the mutant S proteins or whether the wild-type S protein adopts the same strategy remains to be determined. However, the first hydrophobic region of S clearly possesses signal function as this region alone was shown to be sufficient for translocation of homologous (11) and heterologous (12) sequences across ER membranes in a cell-free system.

Interestingly, even deletion of both the first hydrophobic and hydrophilic domains of S still allows membrane anchoring and translocation of (at least) the second hydrophilic loop carrying the conformational antigen and the glycosylation site. Thus, our data demonstrate that the entire N-terminal third (aa 1 to 74) of S is dispensable for the first event in HBsAg transport.

Conversely, the subsequent step in this pathway seems to require this region since the capacity of mutants Δ01-74 and Δ10-72 to interact with wild-type S or a modified version of S carrying a foreign epitope was significantly impaired. This indicates that the N-terminal third of S may be directly involved in intermolecular subunit recognition. Mutants carrying smaller lesions in this region retained their ability for oligomerization, thereby exerting a dominant inhibitory effect on the secretion of wild-type S. In this respect, the phenotype of mutant Δ10-32, devoid of the N-terminal signal sequence, differs from that of an analogous deletion mutant of the HBV adw2 subtype which was found to be completely aggregation deficient (5). In contrast, none of the secretion-defective mutants affected export of the mouse T-cell growth factor IL-9 when coexpressed in the same cell. Therefore, specific interaction between mutant and wild-type S chains most likely accounts for the block to secretion of wild-type S.

Since the secretion-defective deletion mutants which were still competent for oligomerization failed to form soluble lipoprotein particles, we conclude that these mutants were arrested in the budding process during particle maturation. Mechanical disruption of cells transfected with the wild-type S gene combined with mild centrifugal forces has been shown to yield two populations of the S protein: aqueous-nonextractable S polypeptides present in the particulate fraction and soluble S proteins (23, 27). As judged by density and sedimentation velocity analysis (7, 23, 38; this work) and electron microscopy (23), S proteins present in the soluble fraction resemble secreted HBsAg lipoprotein particles. The cell-associated assembled S proteins were most likely released from the lumen of the ER or a pre-Golgi compartment because of the disruption of internal membranes. According to the molecular weight of the glycosylated forms of these particles, oligosaccharide processing to the complex form has still not occurred. Conversely, the secretion-defective mutants analyzed in this work were exclusively found in the particulate fraction of transfected cells. In addition, we have observed a strong but not absolute correlation between the secretion competence of various mutant S proteins and their appearance in the soluble fraction using the fractionation scheme employed in this work (unpublished results). Taken together, these data support the notion that the secretion-defective mutant S proteins remained arrested in a particulate, membrane-associated configuration. However, the precise conformation of these proteins requires further analysis. In this respect, our data are not in accord with the results of a mutational analysis of the S protein performed with yeast cells (1). Araki et al. (1) observed that elimination of aa 21 to 80 of the S protein decreased but did not abolish particle-forming ability as judged by velocity sedimentation and electron microscopy of detergent-extracted proteins. Since yeast cells do not secrete HBsAg particles, differences in the assembly of subviral particles in yeast and animal cells may account for the observed discrepancy.

It is now widely held that correct folding of monomeric proteins and proper assembly of oligomeric structures are prerequisites for the exit of secretory proteins from the ER (20). Therefore, it seems likely that the oligomerization- or assembly (budding)-defective S deletion mutants analyzed in this work were retained in the ER. Their sensitivity to digestion with endo H supports this assumption. Protein degradation in the ER has been shown to be involved in the disposal of transport-incompetent proteins (21). The varying intracellular amounts of the secretion-deficient S deletion mutants may be due to differential rates of ER degradation.

Various viral envelope proteins have been used as models for studying assembly, processing, and transport of oligomeric proteins through the exocytic pathway of eukaryotic cells. Generally, intracellular transport of these viral envelope proteins is arrested in the compartment where virion assembly (i.e., interaction with the viral nucleocapsid) occurs (37). The small S envelope protein of HBV shares structural motifs with other viral envelope proteins spanning the lipid bilayer several times, e.g., the E1 envelope protein of coronavirus (2, 28). However, the S protein is distinguished by two prominent features from the majority of the other viral envelope proteins. First, the S protein escapes from assembly into virions, leaving the infected cells in the form of empty envelopes unless retained through the related large envelope protein of HBV (22, 30, 32, 38). And second, the empty envelope is a complex structure that seems to lack a typical unit membrane organization (41) and has a lipid content much lower than that of most cellular membranes (15, 39). Therefore, the panel of oligomerization-competent

but assembly-deficient S deletion mutants characterized in this work should be helpful tools to analyze the unique but still unknown budding mechanism of HBsAg particles.

In some respects, HBsAg particles resemble liver-derived lipoproteins crucial for the transport of lipids. Apolipoprotein B100 is the quantitatively dominant protein component of the very low density and low-density lipoprotein particles (6). Although the precise assembly pathway of these particles also remains to be elucidated, it has been proposed that integration of apolipoprotein B100 into the membrane of the ER provides a mechanism through which this protein can extract membrane lipids and assemble them into lipoprotein particles (6). It is therefore tempting to speculate that HBsAg particle assembly follows a similar strategy.

To conclude, the mutants described in this work and the various experimental approaches used allowed us to monitor and to dissect different steps in the biogenesis of the HBV envelope, i.e., association of S proteins with membranes, translocation across the ER membrane, aggregation of monomers, and assembly of soluble lipoprotein particles. However, important features of these steps, as well as the subsequent stages of the transport along the exocytic pathway, still remain enigmatic. Further experiments using the approach employed in this work should provide additional insights in the maturation of HBsAg particles.

## ACKNOWLEDGMENTS

We are grateful to G. Lutfalla for the HepG2 HGPRT$^-$ cell line, B. Fleischer for the COS-7 cells, F. Delpeyroux for providing plasmids pLAS and pBAP and monoclonal antibody C3, and E. Schmitt for cloned IL-9 cDNA. We gratefully acknowledge the perfect technical assistance of A. Clemen. We also thank U. Machein for photographic work, R. Hilfrich for experimental support, and S. Goedert for performing the T-cell proliferation assays.

This work was supported by the Deutsche Forschungsgemeinschaft (Sonderforschungsbereich 311) and by the Naturwissenschaftlich-Medizinisches Forschungszentrum of the University of Mainz.

## REFERENCES

1. **Araki, K., K. Shiosaki, M. Araki, O. Chisaka, and K. Matsubara.** 1990. The essential region for assembly and particle formation in hepatitis B virus surface antigen produced in yeast cells. Gene **89:**195–201.
2. **Armstrong, J., H. Niemann, S. Smeekens, P. Rottier, and G. Warren.** 1984. Sequence and topology of a model intracellular membrane protein, E1 glycoprotein, from a coronavirus. Nature (London) **308:**751–752.
3. **Bormann, B.-J., W. J. Knowles, and V. T. Marchesi.** 1989. Synthetic peptides mimic the assembly of transmembrane glycoproteins. J. Biol. Chem. **264:**4033–4037.
4. **Boyd, D., and J. Beckwith.** 1990. The role of charged amino acids in the localization of secreted and membrane proteins. Cell **62:**1031–1033.
5. **Bruss, V., and D. Ganem.** 1991. Mutational analysis of hepatitis B surface antigen particle assembly and secretion. J. Virol. **65:**3813–3820.
6. **Davis, R. A., R. N. Thrift, C. C. Wu, and K. E. Howell.** 1990. Apolipoprotein B is both integrated into and translocated across the endoplasmic reticulum membrane. J. Biol. Chem. **265:**10005–10011.
7. **Delpeyroux, F., N. Chenciner, A. Lim, M. Lambert, Y. Malpièce, and R. E. Streeck.** 1987. Insertions in the hepatitis B surface antigen. J. Mol. Biol. **195:**343–350.
8. **Delpeyroux, F., N. Chenciner, A. Lim, Y. Malpièce, B. Blondel, R. Crainic, S. van der Werf, and R. E. Streeck.** 1986. A poliovirus neutralization epitope expressed on hybrid hepatitis B surface antigen particles. Science **233:**472–475.
9. **Delpeyroux, F., E. van Wezel, B. Blondel, and R. Crainic.** 1990. Structural factors modulate the activity of antigenic poliovirus sequences expressed on hybrid hepatitis B surface antigen particles. J. Virol. **64:**6090–6100.
10. **Eble, B. E., V. R. Lingappa, and D. Ganem.** 1986. Hepatitis B surface antigen: an unusual secreted protein initially synthesized as a transmembrane polypeptide. Mol. Cell. Biol. **6:**1454–1463.
11. **Eble, B. E., V. R. Lingappa, and D. Ganem.** 1990. The N-terminal (pre-S2) domain of a hepatitis B virus surface glycoprotein is translocated across membranes by downstream signal sequences. J. Virol. **64:**1414–1419.
12. **Eble, B. E., D. R. MacRae, V. R. Lingappa, and D. Ganem.** 1987. Multiple topogenic sequences determine the transmembrane orientation of hepatitis B surface antigen. Mol. Cell. Biol. **7:**3591–3601.
13. **Galibert, F., E. Mandart, F. Fitoussi, P. Tiollais, and P. Charnay.** 1979. Nucleotide sequence of the hepatitis B virus genome (subtype ayw) cloned in E. coli. Nature (London) **281:**646–650.
14. **Ganem, D.** 1991. Assembly of hepadnaviral virions and subviral particles. Curr. Top. Microbiol. Immunol. **168:**61–83.
15. **Gavilanes, F., J. M. Gonzalez-Ros, and D. L. Peterson.** 1982. Structure of hepatitis B surface antigen. J. Biol. Chem. **257:**7770–7777.
16. **Guerrero, E., F. Gavilanes, and D. L. Peterson.** 1988. Model for the protein arrangement in HBsAg particles based on physical and chemical studies, p. 603–613. *In* A. J. Zuckerman (ed.), Viral hepatitis and liver disease. Alan R. Liss, Inc., New York.
17. **Heermann, K. H., U. Goldmann, W. Schwartz, T. Seyffarth, H. Baumgarten, and W. H. Gerlich.** 1984. Large surface proteins of hepatitis B virus containing the pre-*s* sequence. J. Virol. **52:**396–402.
18. **Horten, R. M., H. D. Hunt, S. N. Ho, J. K. Pullen, and L. R. Pease.** 1989. Engineering hybrid genes without the use of restriction enzymes: gene splicing by overlap extension. Gene **77:**61–68.
19. **Howard, C. R., H. J. Stirk, S. E. Brown, and M. W. Steward.** 1988. Towards the development of synthetic hepatitis B vaccines, p. 1094–1101. *In* A. J. Zuckerman (ed.), Viral hepatitis and liver disease. Alan R. Liss, Inc., New York.
20. **Hurtley, S. M., and A. Helenius.** 1989. Protein oligomerization in the endoplasmic reticulum. Annu. Rev. Cell Biol. **5:**277–307.
21. **Klausner, R. D., and R. Sitia.** 1990. Protein degradation in the endoplasmic reticulum. Cell **62:**611–614.

21a. **Klensch, C., C. Mangold, and R. E. Streeck.** Unpublished results.

22. **Kuroki, K., R. Russnak, and D. Ganem.** 1989. Novel N-terminal amino acid sequence required for retention of a hepatitis B virus glycoprotein in the endoplasmic reticulum. Mol. Cell. Biol. **9:**4459–4466.
23. **Lanford, R. E., V. Luckow, R. C. Kennedy, G. R. Dreesman, L. Notvall, and M. D. Summers.** 1989. Expression and characterization of hepatitis B virus surface antigen polypeptides in insect cells with a baculovirus expression system. J. Virol. **63:**1549–1557.
24. **Lipp, J., and B. Dobberstein.** 1988. Signal and membrane anchor function overlap in the type II membrane protein IγCat. J. Cell Biol. **106:**1813–1820.
25. **Lipp, J., N. Flint, M.-T. Haeuptle, and B. Dobberstein.** 1989. Structural requirements for membrane assembly of proteins spanning the membrane several times. J. Cell Biol. **109:**2013–2022.
26. **Lutfalla, G., L. Armbruster, S. Dequin, and R. Bertolotti.** 1989. Construction of an EBNA-producing line of well differentiated human hepatoma cells and of appropriate Epstein-Barr virus-based shuttle vectors. Gene **76:**27–39.
27. **Marquardt, O., K. H. Heermann, M. Seifer, and W. H. Gerlich.** 1987. Cell-type dependent expression and secretion of hepatitis B virus pre-S1 surface antigen. Postgrad. Med. J. **63:**41–50.
28. **Mayer, T., T. Tamura, M. Falk, and H. Niemann.** 1988. Membrane integration and intracellular transport of the coronavirus glycoprotein E1, a class III membrane glycoprotein. J. Biol. Chem. **263:**14956–14963.
29. **McGovern, K., M. Ehrmann, and J. Beckwith.** 1991. Decoding

signals for membrane protein assembly using alkaline phosphatase fusions. EMBO J. **10**:2773–2782.
30. **McLachlan, A., D. R. Milich, A. K. Raney, M. G. Riggs, J. L. Hughes, J. Sorge, and F. V. Chisari.** 1987. Expression of hepatitis B virus surface and core antigens: influence of pre-S and precore sequences. J. Virol. **61**:683–692.
31. **Nakamaye, K. L., and F. Eckstein.** 1986. Inhibition of restriction endonuclease NciI cleavage by phosphorothioate groups and its application to oligonucleotide-directed mutagenesis. Nucleic Acids Res. **14**:9679–9698.
32. **Ou, J.-H., and W. J. Rutter.** 1987. Regulation of secretion of the hepatitis B virus major surface antigen by the preS-1 protein. J. Virol. **61**:782–786.
33. **Parks, G. D., and R. A. Lamb.** 1991. Topology of eukaryotic type II membrane proteins: importance of N-terminal positively charged residues flanking the hydrophobic domain. Cell **64**:777–787.
34. **Paterson, R. G., and R. A. Lamb.** 1990. Conversion of a class II integral membrane protein to a soluble and efficiently secreted protein: multiple intracellular and extracellular oligomeric and conformational forms. J. Cell Biol. **110**:999–1011.
35. **Patzer, E. J., G. R. Nakamura, C. C. Simonsen, A. D. Levinson, and R. Brands.** 1986. Intracellular assembly and packaging of hepatitis B surface antigen particles occur in the endoplasmic reticulum. J. Virol. **58**:884–892.
36. **Patzer, E. J., G. R. Nakamura, and A. Yaffe.** 1984. Intracellular transport and secretion of hepatitis B surface antigen in mammalian cells. J. Virol. **51**:346–353.
37. **Pettersson, R. F.** 1991. Protein localization and virus assembly at intracellular membranes. Curr. Top. Microbiol. Immunol. **170**:67–106.
38. **Prange, R., A. Clemen, and R. E. Streeck.** 1991. Myristylation is involved in intracellular retention of hepatitis B virus envelope proteins. J. Virol. **65**:3919–3923.
39. **Satoh, O., M. Umeda, H. Imai, H. Tunoo, and K. Inoue.** 1990. Lipid composition of hepatitis B virus surface antigen particles and the particle-producing human hepatoma cell lines. J. Lipid Res. **31**:1293–1300.
40. **Schmitt, E., H. U. Beuscher, C. Huels, P. Monteyne, R. van Brandwijk, J. van Snick, and E. Ruede.** 1991. IL-1 serves as a secondary signal for IL-9 expression. J. Immunol. **147**:3848–3854.
41. **Simon, K., V. R. Lingappa, and D. Ganem.** 1988. Secreted hepatitis B surface antigen polypeptides are derived from a transmembrane precursor. J. Cell Biol. **107**:2163–2168.
42. **Skelly, J., C. R. Howard, and A. J. Zuckerman.** 1981. Hepatitis B polypeptide vaccine preparation in micelle form. Nature (London) **290**:51–54.
43. **Streeck, R. E., A. Clemen, U. Machein, R. Nagel, B. Zahn, F. Delpeyroux, C. Mangold, and R. Prange.** 1991. Analysis of HBsAg assembly and secretion using site-directed mutagenesis, p. 155–159. *In* F. B. Hollinger, S. M. Lemon, and H. S. Margolis (ed.), Viral hepatitis and liver disease. The Williams & Wilkins Co., Baltimore.
44. **Tiollais, P., C. Pourcel, and A. Dejean.** 1985. The hepatitis B virus. Nature (London) **317**:489–495.
45. **van Snick, J., A. Goethals, J.-C. Renauld, E. van Roost, C. Uyttenhove, M. R. Rubira, R. L. Moritz, and R. J. Simpson.** 1989. Cloning and characterization of a cDNA for a new mouse T cell growth factor (P40). J. Exp. Med. **169**:363–368.
46. **von Heijne, G.** 1986. The distribution of positively charged residues in bacterial inner membrane proteins correlates with the trans-membrane topology. EMBO J. **5**:3021–3027.
47. **von Heijne, G.** 1989. Control of topology and mode of assembly of a polytopic membrane protein by positively charged residues. Nature (London) **341**:456–458.
48. **Wigler, M., S. Silverstein, L. S. Lee, A. Pellicier, Y. C. Cheng, and R. Axel.** 1977. Transfer of purified herpes virus thymidine kinase gene to cultured mouse cells. Cell **11**:223–232.
49. **Zerial, M., D. Huylebroeck, and H. Garoff.** 1987. Foreign transmembrane peptides replacing the internal signal sequence of transferrin receptor allow its translocation and membrane binding. Cell **48**:147–155.